



A pilot study of intraoperative localization of peripheral small pulmonary tumors by cone-beam computed tomography: sandwich marking technique

Yuichi Saito^{1,2^}, Tomohiro Watanabe¹, Yasuyuki Kanamoto¹, Momoko Asami¹, Fumi Yokote¹, Hitoshi Dejima¹, Hiroaki Morooka², Takayuki Ibi², Yoshikane Yamauchi^{1^}, Nobumasa Takahashi², Tomohiko Ikeya², Yukinori Sakao^{1^}, Masafumi Kawamura^{1^}

¹Department of Surgery, Teikyo University School of Medicine, Tokyo, Japan; ²Department of Thoracic Surgery, Saitama Cardiovascular and Respiratory Center, Saitama, Japan

Contributions: (I) Conception and design: Y Saito; (II) Administrative support: N Takahashi; (III) Provision of study materials or patients: T Watanabe, Y Kanamoto, M Asami, F Yokote, H Dejima, H Morooka, T Ibi, Y Yamauchi; (IV) Collection and assembly of data: Y Saito, N Takahashi; (V) Data analysis and interpretation: Y Saito; (VI) Manuscript writing: All authors; (VII) Final approval of manuscript: All authors.

Correspondence to: Yuichi Saito. Department of Surgery, Teikyo University School of Medicine, 2-11-1 Kaga, Itabashi-ku, Tokyo 173-8605, Japan. Email: k3699004@gmail.com.

Background: Intraoperative identification of small pulmonary nodules has been an important technical issue. We aimed to develop a new localization method which is much safer and simple procedure compared with conventional methods.

Methods: This was a retrospective study including patients with resected peripheral pulmonary nodules between November 2017 and April 2021 at Teikyo University School of Medicine, and Saitama Cardiovascular and Respiratory Center. All surgical procedure was wedge resection, and the tumor size was equal to or less than 20 mm which were detected by cone-beam computed tomography (CBCT; Philips Allura Xper FD 20, Philips). Some metal clips were put on several places of visceral pleura, where the target lesion was sandwiched by marking clips (sandwich marking technique). CBCT detected both the target lesion and metal clips, and video-assisted thoracoscopic surgery (VATS) was performed. Radiological and pathological findings were analyzed, and the correlation coefficient of tumor size was examined among pre-, intra-, and post-operative tumor sizes.

Results: The average age of 90 patients was 65.2 years, and 47 were male (52.2%). All procedure was wedge resection including twelve bi-wedge resections, and one hundred nine peripheral pulmonary lesions were obtained by sandwich marking technique. The detection rate was 100%, and there was no marking-related complication.

Conclusions: All small peripheral pulmonary lesions were successfully detected and resected by using CBCT with no marking-related complication. Sandwich marking technique was demonstrated to provide safe, reliable, and simple localization procedure for small peripheral pulmonary lesions.

Keywords: Lung cancer; localization; small pulmonary nodules; cone-beam computed tomography (CBCT); video-assisted thoracoscopic surgery (VATS)

Submitted Feb 13, 2022. Accepted for publication May 19, 2022.

doi: 10.21037/jtd-22-190

View this article at: <https://dx.doi.org/10.21037/jtd-22-190>

[^] ORCID: Yuichi Saito, 0000-0002-2025-9226; Yoshikane Yamauchi, 0000-0002-3374-2399; Yukinori Sakao, 0000-0002-6826-2280; Masafumi Kawamura, 0000-0002-5566-8046.

Introduction

Lung cancer, accounting for 2.09 million new cases and 1.76 million deaths according to GLOBOCAN 2018, is the most common cancer and a leading cause of death from cancer in many developed countries (1). Recently, the National Lung Screening Trial reported on the efficacy of low-dose computed tomography (LDCT) screening in reducing lung cancer mortality in the United States, moreover, the Dutch-Belgian lung cancer screening trial (NELSON study) demonstrated that lung cancer mortality in high-risk patients was significantly lower in the CT-screening cohort than in the no-screening cohort (2,3). Hence, the current guidelines highly recommended screening with LDCT to reduce lung cancer-related mortality (4).

With the increasing practice of LDCT screening, thoracic surgeons are increasingly treating patients with small pulmonary nodules that are otherwise invisible on conventional chest roentgenograms. Instead of depending on the tactile sensation of the surgeons' fingers, several preoperative CT-guided marking methods using a needle became widespread in the 1990s. Of these, metal hook-wire placement was widely used as a marker material in preoperative CT (5). This method was effective for localization, but serious complications such as dislodging and migration of the wire, air embolism, bleeding, and pneumothorax were reported (6). Hasegawa *et al.* reported the utility of a dye marker using a mixture of indigo carmine and lipiodol (MIL), which was injected near the pulmonary lesion using a 23-gauge needle before video-assisted thoracoscopic surgery (VATS) (7). Although a 100% detection rate was recorded, five patients with pneumothorax (n=3) and aspiration (n=2) required further interventions. Furthermore, stains are unsuitable for an emphysematous lung because they tend to spread and disappear within the affected lung parenchyma.

To overcome the adverse events of percutaneous needle marking, a bronchoscopic marking method was developed using a barium mixture, dye, and microcoil (8,9). Such bronchoscopy-assisted localization techniques with no percutaneous puncture have evolved in the past, and have helped overcome severe complications such as air embolism. However, their use is limited currently because of the requirement of advanced technology and increased time to prepare and learn to perform accurate mapping. In addition, intraoperative adhesion can make the confirmation of the marker material difficult.

Currently, cone-beam computed tomography (CBCT)

has been used for intraoperative localization for small nodules in a hybrid operating room (hybrid-OR), and a few reported on the use of CBCT-guided VATS with percutaneous localization of a hook-wire, dye-localization, microcoil, or dual-marker (microcoil and dye) (10-12). Rouzé *et al.* advocated non-invasive guidance using intraoperative CBCT and augmented fluoroscopy for pulmonary resection by VATS, which method needed no marker (13). During the anesthesiologist controlled pulmonary ventilation to keep moderate pneumothorax of the affected lung, CBCT scan was performed for the reconstruction imaging which allowed to locate precisely the pulmonary lesion. Afterwards, a 3D reconstruction of the pulmonary nodule was created using a segmentation software (iPilot dynamic function, MMWP station, Siemens Healthcare). A projection of the lesion was made usual fluoroscopic acquisitions. If the localization was failed, the procedure was cancelled and rescheduled with other alternative method (e.g., hook-wire). Alvarez *et al.* also proposed another marker-less localization method using a preoperative image and two intraoperative CBCT images (14). CBCT scan was performed two times due to obtain images of the inflated lung before pneumothorax and of the deflated lung after pneumothorax. Through comparing between those images, biomechanical simulations were conducted to provide an estimation of the intraoperative localization of the target lesion. Anayama *et al.* suggested simultaneous bronchoscopic dye marking and CBCT-guided VATS in a hybrid-OR (15). These intraoperative localization methods using CBCT are developing rapidly, but are considered invasive (percutaneous marking) or highly sophisticated (bronchoscopic marking etc.). Therefore, we aimed to develop a safer, simpler, more accurate marking method for the detection of small lung nodules. We present the following article in accordance with the STROBE reporting checklist (available at <https://jtd.amegroups.com/article/view/10.21037/jtd-22-190/rc>).

Methods

Study design

This study was performed in accordance with the Declaration of Helsinki (as revised in 2013). This was a retrospective study approved by the Institutional Review Board of Teikyo University School of Medicine (approval No. 20-068) and Saitama Cardiovascular and Respiratory Center (approval No. 2020046). Written informed consent

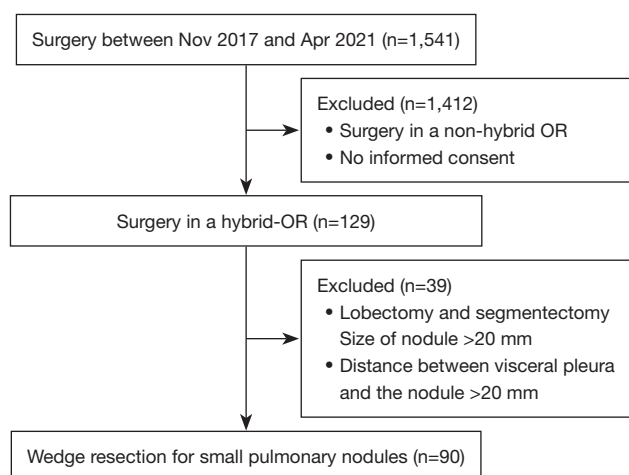


Figure 1 Flowchart of patient enrolment. After collecting all surgery in a hybrid operating room, we enrolled only cases or wedge resection which met the size criteria; (I) tumor size ≤ 20 mm and (II) distance between tumor and nearest visceral pleura ≤ 20 mm. OR, operating room.

was obtained from all patients participating in this study. Clinical data and specimens were collected from the electronic medical records and resected pulmonary tissues of patients at Teikyo University School of Medicine and Saitama Cardiovascular and Respiratory Center. After collecting data of patients who underwent surgery from November 2017 to April 2021, we selected cases requiring intraoperative localization in a hybrid OR (Figure 1). Finally, case of wedge resection for pulmonary lesions both with tumor size ≤ 20 mm and with distance ≤ 20 mm from nearest visceral pleura on preoperative multi-detector CT (MDCT; Aquilion ONE TSX-301C320, Toshiba, Japan) were enrolled into this study. The three primary end points of the study were (I) identification rate by CBCT (Allura Xper FD20, Phillips, The Netherlands), (II) pathological negative rate of surgical stump, and (III) exposure dose measurement by a wearable dosimeter (nanoDot®; Nagase Landauer, Tsukuba, Japan).

Surgical indications for peripheral small lung tumor

According to our policy, peripheral small pulmonary nodules should be resected surgically when the lesion presents the following malignant features: (I) suspicious malignancy of pulmonary lesion, and (II) pulmonary lesion size 2–20 mm. Furthermore, intraoperative localization by CBCT in a hybrid-OR is recommended when the distance

between the pulmonary lesion and nearest visceral pleura is 20 mm or less, and when the lesion is resectable by VATS. When a pulmonary lesion was deep intralobar or mediastinal pleura, wedge resection was contraindicated because it was difficult to secure the surgical margin. No patient was arbitrary excluded, but an alternative marking method such as preoperative percutaneous dye marking is used if a hybrid-OR is not available on the operation day (7).

Skin marking in a hybrid-OR

All patients had neither a marking nor pathological diagnosis prior to the surgery. The hybrid-OR was equipped with a CBCT scanner and a free-floating table (Maquet Co., Ltd., Germany). Patients were administered general anesthesia and were intubated with a double-lumen endobronchial tube in the supine position. After they were repositioned into the lateral decubitus position, two or more metal clips were placed on the body surface where the target lesion could be located directly, with reference to the preoperative multi-detector computed tomography (MDCT) images (Figure 2A). Subsequently, CBCT was performed during an end inspiration breath-hold using a standard 10-s CBCT protocol to identify the positional relationship among the clips and the pulmonary target lesion (Figure 2B). Next, the nearest skin surface from the lesion was marked with the help of the CBCT image (Figure 2C). The body surface marking was not mandatory in the case of pulmonary lesions which were not able to approached directly, for instance under scapula, apex, above diaphragm, etc.

Sandwich marking technique

Three-port VATS was performed for the identification and pulmonary resection of small lung tumors. Using preoperative MDCT and CBCT images (Figure 2A–2C), the first VATS port was made above the target lesion in the lung due to challenge to touch with fingers. In non-palpable cases, the lesion's location was estimated based on the proximity between the first VATS port and the lesion. It was needed to inflate the affected lung up to the maximum and to achieve no atelectasis for detecting any small or ground-glass opacity lesions during CBCT imaging. Thereafter, two or three locations on the visceral pleura were marked to sandwich the expected location of the pulmonary lesion using a metal clip (Ligaclip ER420®, Ethicon, Co., Ltd., Japan) (Figure 2D). Ideally, the clipping was performed by

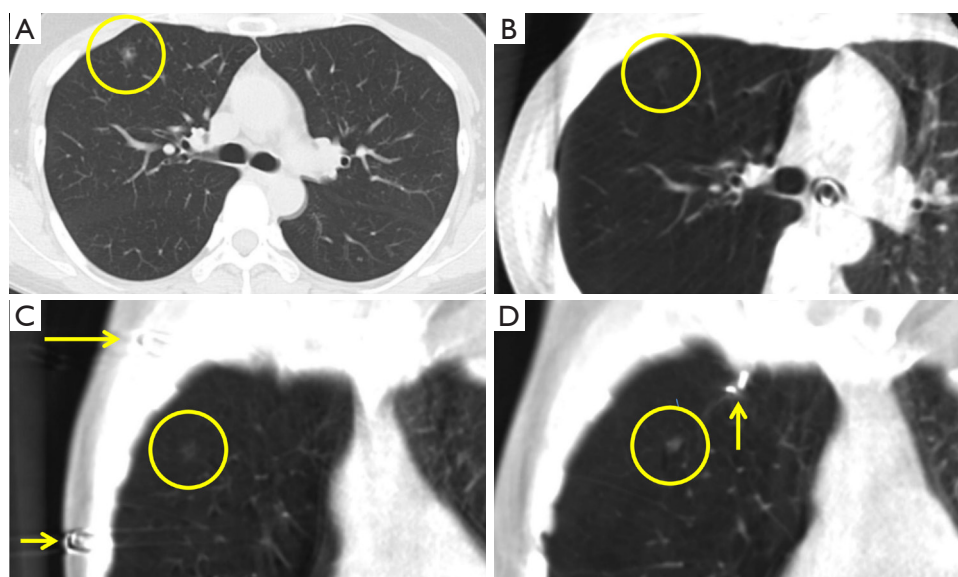


Figure 2 Case presentation of small ground-glass opacity in the right upper lobe of the lung. Small pulmonary nodule was detected by MDCT, preoperatively (A). In the hybrid operating room, it was also confirmed by CBCT (B). It was possible to know the positional relation between the target lesion and skin marking on the CBCT monitor before surgery (C). Similarly, we were able to know the positional relation between the target lesion and some metal clips on visceral pleura by CBCT imaging during surgery (D). CBCT imaging and pleural marking can be performed repeatedly until the target lesion is localized exactly. In summary, CBCT was inferior to MDCT at the time of qualitative diagnosis, but it had sufficient performance of presence diagnosis, intraoperatively. MDCT, multi-detector computed tomography; CBCT, cone-beam computed tomography. Note that arrows indicate metal clips, and circles surround a pulmonary lesion.

maintaining a distance of approximately 30 mm from the target lesion to ensure the distance of the surgical stump (Figure 3A,3B), and the target should be sandwiched by two or three markings (Figure 3C). CBCT scan can be repeated for understanding the position exactly. After successful localization of the lesion, VATS wedge resection was performed with an endostapler under the guidance of the metal clips (Figure 3D). It was noted carefully to keep the distance, about 30 mm, between the target lesion and a marker clip due to ensure surgical margin. All unnecessary clips were removed by the forceps before wedge resection, and wedge resection was performed including all marker clips. As needed, any injured visceral pleura was repaired by suture or resected by endostapler.

Wearable dosimeter

To determine skin radiation exposure, 5 wearable dosimeters were attached at each intercostal space in the opposite middle axillary line (Figure 4A). The third dosimeter was just put on the other side of pulmonary lesion, where was displayed with point zero in Figure 4B. Theoretically, those

dosimeters measured skin exposure dose including scattered radiation not only within the field of view (FOV) but also out of the FOV in CBCT. Likewise, we measured skin radiation exposure by MDCT as a control for one patient. Furthermore, two pulmonary markings were performed using MIL before VATS by the Lipiodol marking method and skin radiation exposure of the patients attached with five dosimeters was measured during the entire period (at the time of both preoperative CT fluoroscopy for injecting MIL and intraoperative fluoroscopy for localization of dye pigmentation near the pulmonary lesion (7).

Statistical analysis

Descriptive statistics and categorical variables were computed using standard formulae with Excel 2019 ver. 16.0.12527.20260® (Microsoft Corp, Tokyo, Japan) and SPSS Statistics® version 27 (IBM Corp., Armonk, NY, USA). Scatter plot and correlation coefficient analyses were performed using the statistical software R version 3.6.3 (R Foundation for Statistical Computing, Vienna, Austria) with psych package. $P < 0.05$ was considered statistically

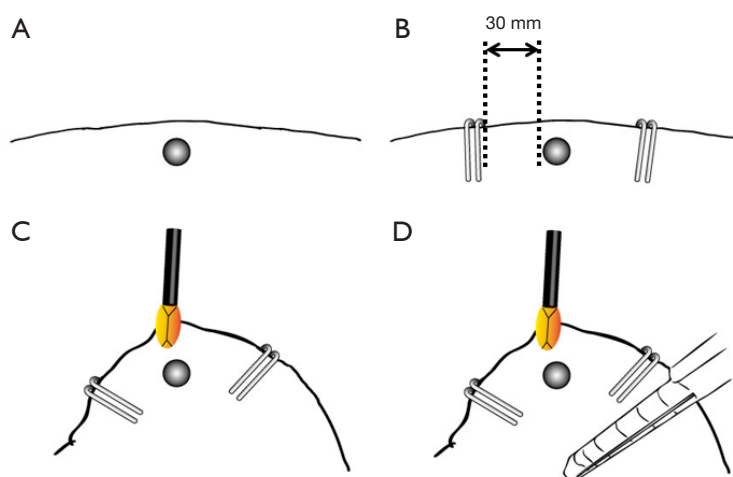


Figure 3 Sandwich marking technique is explained by Figure 3. Peripheral pulmonary lesion is detected by CBCT (A). Several places on the visceral pleura are marked with a metal clip (Ligaclip ER420®, Ethicon, Co., Ltd., Japan), and the distance between the lesion and nearest visceral pleura should be more 30 mm (B). After CBCT reconfirmation of the localization, surgical resection line can be decided by referring metal clips (C). Wedge resection can be performed with an endostapler under the guidance of the metal clips (D). The sufficient distance between the tumor and metal clips allows us to secure enough surgical margin. CBCT, cone-beam computed tomography.

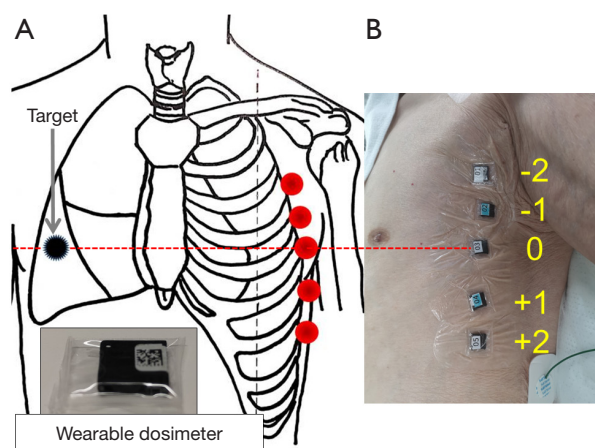


Figure 4 Five wearable dosimeters were put on the body of patients who had wedge resection in a hybrid operating room. Those dosimeters were attached on the opposite middle axillary line from the target (A). The middle dosimeter was located at the same level of the target lesion (zero position). In this case, tumor was located in the lower lobe of the lung, and 3rd dosimeter (center dosimeter) was put on 5th intercostal space on left middle axillary line. First and 5th dosimeters were found at 3rd and 5th intercostal space, respectively (B demonstrated “-2” and “+2”).

significant. If data was missing for more than 90% of the clinicopathological variables, the case was excluded from this study.

Results

Patient characteristics

Patient characteristics and surgical data are presented in Table 1. All case had sufficient data of clinicopathological variables. The mean age of the patients was 65.2 years (25–83 years), and most were male (52.2%). The number of pulmonary lesions was 71 (78.9%) in single lesion cases, 17 (18.9%) in double lesion cases, and 2 (2.2%) in multiple lesion cases. The most common surgical procedure was single wedge resection (86.7%). The average durations of surgery and anesthesia were 128 and 206 min, respectively. Average blood loss was 15 mL, and the average number of CBCT scans was 2.7 [1–8], and no complications related to intraoperative localization were noted.

Characteristics of nodules

The side of surgery was right in 60 (55.0%) and left in 49 (45.0%) patients (Table 2). One hundred nine pulmonary lesions were detected in 90 patients by CBCT and were completely resected by VATS. Among these, 52 lesions were in the lower lobe (47.7%), 50 in the upper lobe (45.9%), and 7 (6.4%) in the middle lobe. The average tumor size was 9.6 mm (2–20 mm) on multi-detector computed tomography, 9.4 mm (2–20 mm) on CBCT, and 9.7 mm (3–30 mm) in pathology, respectively. Consolidation/Tumor

Table 1 Clinical characteristics of study patients (n=90)

Characteristic	N (%)
Age, years	65.2±13.2
Sex	
Male	47 (52.2)
Female	43 (47.8)
Number of pulmonary lesions	
Single	71 (78.9)
Double	17 (18.9)
Multiple	2 (2.2)
Surgical procedure	
Single wedge resection	78 (86.7)
Bi-wedge resection	12 (13.3)
Intraoperative adhesion	21 (23.3)
Time (surgery, min)	128±52.4
Time (anesthesia, min)	206±55.3
Blood loss (mL)	15.0±32.3
Scan times (min)	2.7±1.17
Complication	0 (0)

Data is presented as mean ± standard deviation or numbers and percentages.

ratio (C/T ratio) demonstrated 53 solid nodules (49.6%), 39 sub-solid nodules (35.8%), and 17 pure ground glass nodule (15.6%) in Table 2. And then, 41 lesions (37.6%) were palpable. Pathological diagnosis revealed 46 primary lung cancers (42.2%), 41 metastatic tumors (37.6%), 5 fibroses (4.6%), 2 infectious diseases (1.8%), and 1 benign tumor (0.9%). The detection rate was 100%, and surgical stump of each lesion was pathologically negative meaning that all lesions were fully resected (R0).

Comparison of tumor size on CBCT, MDCT, and pathological assessment

The scatter plots with each correlation coefficient are demonstrated in Figure 5 for each combination (MDCT, CBCT, and pathological assessment). The size of smallest tumor was 2 mm in solid, 5 mm in sub-solid, and 4 mm in pure ground-glass opacity. Figure 2 demonstrates the representative case of pure ground-glass opacity which size was 8 mm on MDCT image. The correlation coefficient was

Table 2 Characteristics of pulmonary nodules (n=109)

Characteristic	N (%)
Side	
Right	60 (55.0)
Left	49 (45.0)
Lobe	
Upper	50 (45.9)
Middle	7 (6.4)
Lower	52 (47.7)
Tumor size on MDCT (mm)	9.6±4.20
Tumor size on CBCT (mm)	9.0±3.88
Tumor size in pathology (mm)	9.7±5.00
Consolidation/tumor ratio on MDCT	
Solid [1]	53 (49.6)
Sub-solid [>0, <1]	39 (35.8)
Pure ground-glass opacity [0]	17 (15.6)
Pathological diagnosis	
Lung cancer	46 (42.2)
Metastatic tumor	41 (37.6)
Pulmonary fibrosis	5 (4.6)
Infectious disease	2 (1.8)
Benign tumor	1 (0.9)
Other	14 (12.8)
CBCT detection rate	115 (100.0)
Surgical stump	
Negative	109 (100.0)
Positive	0 (0)

Data is presented as mean ± standard deviation or numbers and percentages. MDCT, multi-detector computed tomography; CBCT, cone-beam computed tomography.

0.82 between MDCT and CBCT ($P<0.001$), 0.74 between MDCT and pathological assessment ($P<0.001$), and 0.66 between CBCT and pathological assessment ($P<0.001$).

Skin radiation dose

Wearable dosimeters were used to measure the skin radiation dose of 12 patients in the hybrid-OR and of two patients who underwent the Lipiodol marking method

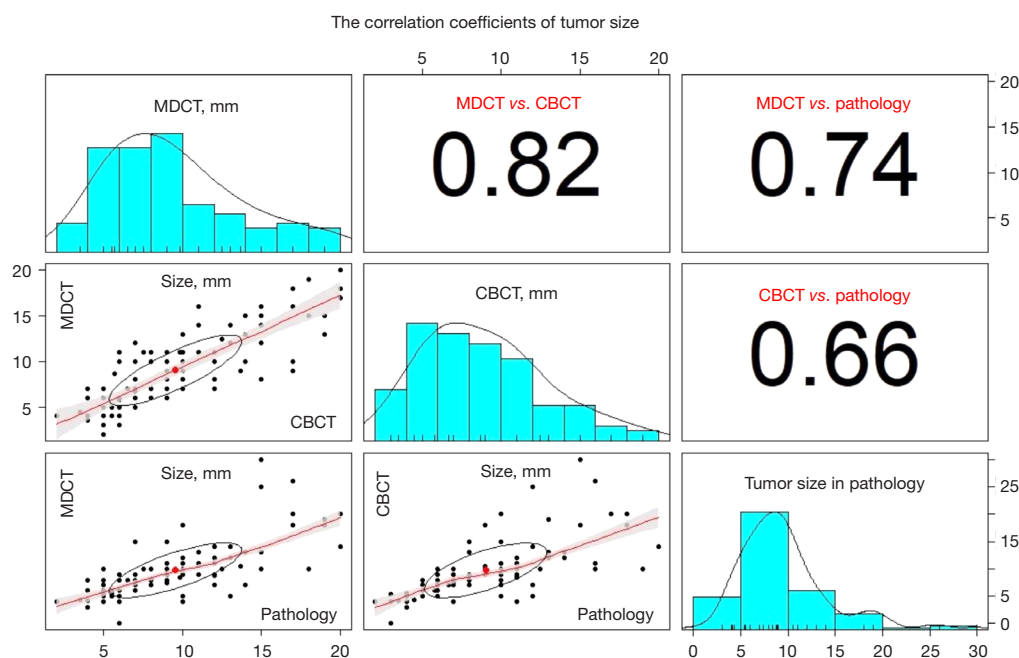


Figure 5 Tumor sizes from MDCT, CBCT, and pathology. Three dot plots and bar plots demonstrate the relationships of tumor size compared with that on another device or in pathology. The correlation coefficients were 0.82 (MDCT *vs.* CBCT), 0.74 (MDCT *vs.* pathology), and 0.66 (CBCT *vs.* pathology), respectively. MDCT, multi-detector computed tomography; CBCT, cone-beam computed tomography.

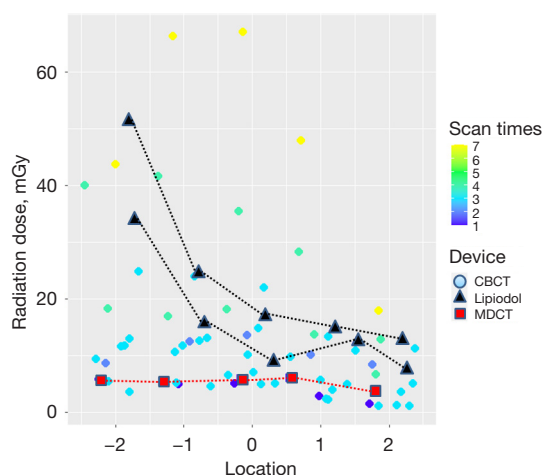


Figure 6 Patient radiation exposure by MDCT, CBCT, and the Lipiodol marking method. The X-axis indicates location (-2, -1, 0, +1, +2), and the median location was at the same level of the target pulmonary nodule. The red square represents skin radiation dose of MDCT, ranging from 3.794 to 6.048 mGy. Moreover, black trigone represents the Lipiodol marking method. Other round dots indicate the location and skin radiation dose of CBCT. MDCT, multi-detector computed tomography; CBCT, cone-beam computed tomography.

(control). The MIL was injected into the lung parenchyma of two patients while using MDCT preoperatively, and the indigo carmine staining was identified by C-arm fluoroscopy (OEC Brivo Essential; GE Healthcare Japan, Tokyo, Japan). The skin radiation doses were measured preoperatively and intraoperatively. Similarly, the skin radiation dose of one patient who underwent MDCT was recorded as the control. In *Figure 6*, the red square shows skin radiation doses at five locations during MDCT; the values ranged from 3.794 to 6.048 mGy. Contrastingly, the skin radiation doses in the Lipiodol marking method ranged from 7.752 to 51.441 mGy (black trigone). According to the dot plots (*Figure 6*), radiation exposure in CBCT is comparable to that in MDCT and less than that in the Lipiodol method if the number of CBCT scan is less than 4 times. Conversely, the skin radiation dose in a hybrid-OR is greater than that in the Lipiodol marking method when the number of CBCT scan is more than 4 times.

Discussion

All small peripheral pulmonary nodules were easily, certainly, and safely resected by the Sandwich Marking

Technique. Intraoperative identification of such a small nodule has been highly challenging for surgeons for a long time; several clinical methodologies for their preoperative or intraoperative localization are known. In the beginning of the 1990s, CT-guided percutaneous hook-wire marking was adopted for preoperative localization of a peripheral pulmonary nodule, but the use of this method has reduced because of the rare but severe complications such as air embolism (6). Other alternative marking methods to percutaneous needle marking have been developed in the last two decades (8,16). With the progress in research of the transbronchial approach, CBCT combined with bronchoscopic marking has resulted in a high detection rate of the target nodule, with no localization-related dissemination complication (17). However, preoperative or intraoperative reduction of the radiation exposure remains a pivotal clinical issue. Furthermore, the complexity of the procedure hinders its widespread dissemination (18).

In 2013, Uneri *et al.* investigated the image-guidance system, CBCT, for localization of a pulmonary lesion using a cadaveric porcine specimen (19). Gill *et al.* reported the results of a phase I-II clinical trial (NCT01847209) in 2015, in which 23 patients underwent intraoperative CBCT-guided percutaneous pulmonary marking followed by VATS resection of the tumor (20). In Japan, 19 small pulmonary nodules were resected in 17 patients under CBCT guidance in a hybrid OR (21). Since then, several reports of dye marking and/or hook-wire marking by CBCT in a hybrid OR have been published (12,22-24). However, CBCT marking with a needle can cause complications such as bleeding, air embolism, and pneumothorax.

Since neither needle nor bronchoscopy was used in sandwich marking technique, it is considered as simpler method compared to the conventional ones. In actuality, a small number of cases were enough for experienced surgeons to learn this technique. In addition, it was proved to be significant accurate because the surgical stumps of all nodules were pathologically negative, and the correlation coefficient was high implying almost the same tumor size between preoperative MDCT and intraoperative CBCT images (*Figure 5*). About the safety, the marking-related complications do not occur theoretically, and it was proved actually in this study. This technique enables repeat markings and confirmation intraoperatively; the average number of CBCT scan was 2.7 (1–8 times), and more than 90% of cases required less than 4 scan times. Therefore, patient radiation exposure met in the tolerance level in most cases. However, there were some reasons why multiple

CBCT scans (≥ 4 times) was required, including failure of sandwich marking/refine localization ($n=8$), multiple target lesions ($n=5$), and/or thoracic adhesion/refine localization ($n=3$). So, it is necessary in near future to conduct a clinical study comparing radiation exposures among various methods for intraoperative localization.

In general, it tends to be considered that small and pure ground glass opacity can be barely visible, or even not visible at all. At first, we were afraid of failing to detect such a difficult lesion before starting this study, but all visualization was achieved for any small lesions through CBCT imaging with no atelectasis in this study (*Figure 2*). Here, it was confirmed that CBCT was able to detect the ground-glass opacity which size was 4 mm.

In this study, mean surgical time included intraoperative marking time, so it was greater than two hours. However, it could be even shorter by smooth cooperation among medical staffs including anesthesiologists, nurses, radiological technicians and surgeons. In addition, it must be noticed that it did not include time for marking in previous literatures about alternative methods. For example, date of surgery after marking procedure demonstrated 1-day (20.8%), 2-day (0.6%), and 3-day (0.6%) (7). In other words, total time from Lipiodol marking to end of surgery was at least over 12 hours in 22.0% of cases in the study.

Similar attention is necessary when comparing patient radiation exposure among different marking methods, because there were few studies investigating it from marking procedure to surgery. And, there is no multicenter clinical trial to compare it among various types of pre- or intraoperative identification methods. In this study, it was measured by wearable dosimeters indicating acceptable range of radiation dose compared to the conventional method (*Figure 6*). In addition, there is no risk of radiation exposure for surgeons, anesthesiologists, and nurses, because they can be outside a hybrid OR during CBCT imaging by radiological technicians.

Our study reveals that localization of small nodules in intraoperative adhesion was definitely achieved (21 cases). This is the robust technique that enables location and resection of impalpable pulmonary nodules even in case of severe intrathoracic adhesions. Additionally, another excellent feature of the current method is that multiple targets can be identified simultaneously by CBCT. This series comprised 19 cases of multiple nodules which were required to be detected intraoperatively. The most important aspect of our method was maintaining a distance of 2–3 cm between pulmonary nodule and metal clips (*Figure 3B*).

We believe it can be technically easy for surgeons to learn to sandwich the target lesion with metal clips on the pleural viscera rather than by marking the nearest location (*Figure 3*). In this study, there was one experienced surgeon (YS) developed this technique and gave instruction in it to other eight surgeons, including three surgical residents.

This study had several limitations: (I) relatively small number of cases; (II) multicenter studies by only two institutes; and (III) no data of statistically accurate comparison of skin radiation exposure between the sandwich marking technique and conventional methods. *Figure 6* illustrates scatter plots of the radiation dose (mGy) at five locations on the patients' skin surface, implying similar exposure doses at all intercostal spaces in CBCT and MDCT. However, the five measured values in our lipiodol marking method (n=2) were different depending on each location. These data suggest that radiation exposure was well controlled in CBCT as well as MDCT, but was scattered in the lipiodol marking method, using preoperative MDCT and intraoperative C-arm fluoroscopy. From these findings, we postulated two essential tentative theories (I) radiation exposure could be tolerant if CBCT scan times are less than 4 and (II) radiation exposure by C-arm fluoroscopy may be difficult to control. Therefore, a future study has been planned to compare radiation exposure among the different marking methods.

In conclusion, our study demonstrates the safety and efficacy of the sandwich marking technique to localize small peripheral pulmonary lesions intraoperatively. As well as other marking methods, this technique is not required clinically for pulmonary lesion in central, intralobar, or mediastinal pleural area, because there is not the choice except the anatomical resection (lobectomy or segmentectomy *et al.*) complete resection of such a lesion. Although the clinical challenge of reducing CBCT scan times and radiation exposure remains, more experience could enable identification of target lesions with fewer scans, thereby reducing the radiation exposure of patients.

Acknowledgments

The authors would like to thank Dr. Masafumi Yamagishi, Mr. Kuniaki Shimizu, Mr. Takayuki Yamashita, and Takahiro Futai for providing excellent technical assistance. We express our gratitude to Mr. Ikuro Kobayashi of Nagase-Landauer, Co. Ltd., Tsukuba, Japan, for measurement of radiation exposure.

Funding: None.

Footnote

Reporting Checklist: The authors have completed the STROBE reporting checklist. Available at <https://jtd.amegroups.com/article/view/10.21037/jtd-22-190/rc>

Data Sharing Statement: Available at <https://jtd.amegroups.com/article/view/10.21037/jtd-22-190/dss>

Peer Review File: Available at <https://jtd.amegroups.com/article/view/10.21037/jtd-22-190/prf>

Conflicts of Interest: All authors have completed the ICMJE uniform disclosure form (available at <https://jtd.amegroups.com/article/view/10.21037/jtd-22-190/coif>). The authors have no conflicts of interest to declare.

Ethical Statement: The authors are accountable for all aspects of the work in ensuring that questions related to the accuracy or integrity of any part of the work are appropriately investigated and resolved. The study was conducted in accordance with the Declaration of Helsinki (as revised in 2013). This study was approved by the Institutional Review Board of Teikyo University School of Medicine (Approval Number: 20-068), and Saitama Cardiovascular and Respiratory Center (Approval Number: 2020046). Written informed consent was obtained from all patients participating in this study. This study outcome will not affect the future management of the patients.

Open Access Statement: This is an Open Access article distributed in accordance with the Creative Commons Attribution-NonCommercial-NoDerivs 4.0 International License (CC BY-NC-ND 4.0), which permits the non-commercial replication and distribution of the article with the strict proviso that no changes or edits are made and the original work is properly cited (including links to both the formal publication through the relevant DOI and the license). See: <https://creativecommons.org/licenses/by-nc-nd/4.0/>.

References

1. Ferlay J, Colombet M, Soerjomataram I, et al. Estimating the global cancer incidence and mortality in 2018: GLOBOCAN sources and methods. *Int J Cancer* 2019;144:1941-53.
2. Aberle DR, Adams AM, Berg CD, et al. Reduced lung-

- cancer mortality with low-dose computed tomographic screening. *N Engl J Med* 2011;365:395-409.
3. de Koning HJ, van der Aalst CM, de Jong PA, et al. Reduced Lung-Cancer Mortality with Volume CT Screening in a Randomized Trial. *N Engl J Med* 2020;382:503-13.
 4. Postmus PE, Kerr KM, Oudkerk M, et al. Early and locally advanced non-small-cell lung cancer (NSCLC): ESMO Clinical Practice Guidelines for diagnosis, treatment and follow-up. *Ann Oncol* 2017;28:iv1-iv21.
 5. Zhang H, Li Y, Yimin N, et al. CT-guided hook-wire localization of malignant pulmonary nodules for video assisted thoracoscopic surgery. *J Cardiothorac Surg* 2020;15:307.
 6. Sakiyama S, Kondo K, Matsuoaka H, et al. Fatal air embolism during computed tomography-guided pulmonary marking with a hook-type marker. *J Thorac Cardiovasc Surg* 2003;126:1207-9.
 7. Hasegawa T, Kuroda H, Sato Y, et al. The Utility of Indigo Carmine and Lipiodol Mixture for Preoperative Pulmonary Nodule Localization before Video-Assisted Thoracic Surgery. *J Vasc Interv Radiol* 2019;30:446-52.
 8. Okumura T, Kondo H, Suzuki K, et al. Fluoroscopy-assisted thoracoscopic surgery after computed tomography-guided bronchoscopic barium marking. *Ann Thorac Surg* 2001;71:439-42.
 9. Miyoshi T, Kondo K, Takizawa H, et al. Fluoroscopy-assisted thoracoscopic resection of pulmonary nodules after computed tomography--guided bronchoscopic metallic coil marking. *J Thorac Cardiovasc Surg* 2006;131:704-10.
 10. Pang X, Xue L, Chen J, et al. A novel hybrid technique for localization of subcentimeter lung nodules. *J Thorac Dis* 2017;9:1107-12.
 11. Hsieh MJ, Fang HY, Lin CC, et al. Single-stage localization and removal of small lung nodules through image-guided video-assisted thoracoscopic surgery. *Eur J Cardiothorac Surg* 2018;53:353-8.
 12. Chao YK, Leow OQY, Wen CT, et al. Image-guided thoracoscopic lung resection using a dual-marker localization technique in a hybrid operating room. *Surg Endosc* 2019;33:3858-63.
 13. Rouzé S, de Latour B, Flécher E, et al. Small pulmonary nodule localization with cone beam computed tomography during video-assisted thoracic surgery: a feasibility study. *Interact Cardiovasc Thorac Surg* 2016;22:705-11.
 14. Alvarez P, Rouzé S, Miga MI, et al. A hybrid, image-based and biomechanics-based registration approach to markerless intraoperative nodule localization during video-assisted thoracoscopic surgery. *Med Image Anal* 2021;69:101983.
 15. Anayama T, Hirohashi K, Okada H, et al. Simultaneous cone beam computed tomography-guided bronchoscopic marking and video-assisted thoracoscopic wedge resection in a hybrid operating room. *Thorac Cancer* 2019;10:579-82.
 16. Sakamoto T, Takada Y, Endoh M, et al. Bronchoscopic dye injection for localization of small pulmonary nodules in thoracoscopic surgery. *Ann Thorac Surg* 2001;72:296-7.
 17. Yang SM, Yu KL, Lin KH, et al. Real-time augmented fluoroscopy-guided lung marking for thoracoscopic resection of small pulmonary nodules. *Surg Endosc* 2020;34:477-84.
 18. Sato M, Nagayama K, Kobayashi M, et al. Virtual-Assisted Lung Mapping 2.0: Preoperative Bronchoscopic Three-Dimensional Lung Mapping. *Ann Thorac Surg* 2019;108:269-73.
 19. Uneri A, Nithiananthan S, Schafer S, et al. Deformable registration of the inflated and deflated lung in cone-beam CT-guided thoracic surgery: initial investigation of a combined model- and image-driven approach. *Med Phys* 2013;40:017501.
 20. Gill RR, Zheng Y, Barlow JS, et al. Image-guided video assisted thoracoscopic surgery (iVATS) - phase I-II clinical trial. *J Surg Oncol* 2015;112:18-25.
 21. Mitsuoka M, Terazaki Y, Okamoto Y, et al. Intraoperative marking of an impalpable pulmonary nodule using the Hybrid OR System. *The Journal of the Japanese Association for Chest Surgery* 2015;29:552-8.
 22. Yang SM, Ko WC, Lin MW, et al. Image-guided thoracoscopic surgery with dye localization in a hybrid operating room. *J Thorac Dis* 2016;8:S681-9.
 23. Chao YK, Wen CT, Fang HY, et al. A single-center experience of 100 image-guided video-assisted thoracoscopic surgery procedures. *J Thorac Dis* 2018;10:S1624-30.
 24. Fumimoto S, Sato K, Koyama M, et al. Combined lipiodol marking and video-assisted thoracoscopic surgery in a hybrid operating room. *J Thorac Dis* 2018;10:2940-7.

Cite this article as: Saito Y, Watanabe T, Kanamoto Y, Asami M, Yokote F, Dejima H, Morooka H, Ibi T, Yamauchi Y, Takahashi N, Ikeya T, Sakao Y, Kawamura M. A pilot study of intraoperative localization of peripheral small pulmonary tumors by cone-beam computed tomography: sandwich marking technique. *J Thorac Dis* 2022;14(8):2845-2854. doi: 10.21037/jtd-22-190